Ko, H-G., Choi, J-H., Park, D. I., Kang, S. J., Lim, C-S., Sim, S-E., Shim, J., Kim, J-I., Kim, S., Choi, T-H., Ye, S., Lee, J., Park, P., Kim, S., Do, J., Park, J., Islam, M. A., Kim, H. J., Turck, C. W., ... Kaang, B-K. (2018). Rapid Turnover of Cortical NCAM1 Regulates Synaptic Reorganization after Peripheral Nerve Injury. *Cell Reports*, *22*(3), 748-759. https://doi.org/10.1016/j.celrep.2017.12.059

Article

Cell Reports

Rapid Turnover of Cortical NCAM1 Regulates Synaptic Reorganization after Peripheral Nerve Injury

Graphical Abstract

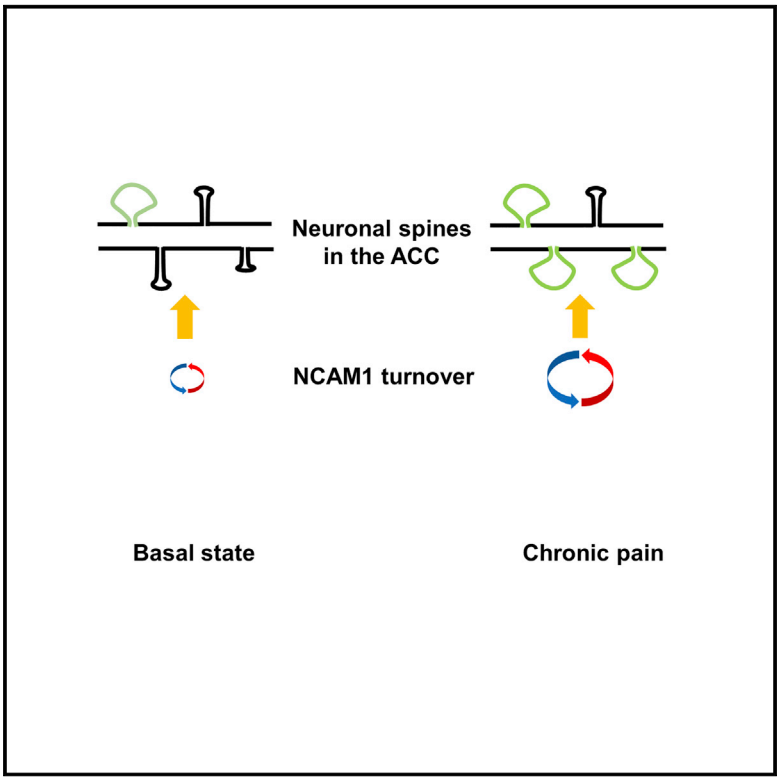

Authors

Hyoung-Gon Ko, Jun-Hyeok Choi, Dong Ik Park, ..., Graham L. Collingridge, Min Zhuo, Bong-Kiun Kaang

Correspondence

g.collingridge@utoronto.ca (G.L.C.), min.zhuo@utoronto.ca (M.Z.), kaang@snu.ac.kr (B.-K.K.)

In Brief

Cortical neuronal circuits reorganize in response to peripheral nerve injury. Ko et al. find that the anterior cingulate cortex (ACC) increases the turnover of specific synaptic proteins after nerve injury. The turnover of neural cell adhesion molecule 1 (NCAM1) mediates spine reorganization and contributes to behavioral sensitization after nerve injury.

Highlights

- Nerve injury causes persistent anatomical and functional changes in the ACC
- Ongoing protein degradation and synthesis are required to sustain ACC alterations
- Inhibition of protein synthesis in the ACC reverses behavioral sensitization
- NCAM1 in the ACC is important for the initiation of behavioral sensitization

Ko et al., 2018, Cell Reports *22*, 748–759
January 16, 2018
https://doi.org/10.1016/j.celrep.2017.12.059

CellPress

OPEN ACCESS
CellPress

Cell Reports
Article

Rapid Turnover of Cortical NCAM1 Regulates Synaptic Reorganization after Peripheral Nerve Injury

Hyoung-Gon Ko,[1,6,8] Jun-Hyeok Choi,[1,8] Dong Ik Park,[2] SukJae Joshua Kang,[1] Chae-Seok Lim,[1] Su-Eon Sim,[1] Jaehoon Shim,[1] Ji-Il Kim,[1] Siyong Kim,[1] Tae-Hyeok Choi,[1] Sanghyun Ye,[1] Jaehyun Lee,[1] Pojeong Park,[1] Somi Kim,[1] Jeehaeh Do,[1] Jihye Park,[1] Md Ariful Islam,[1] Hyun Jeong Kim,[3] Christoph W. Turck,[2] Graham L. Collingridge,[4,5,6,7,*] Min Zhuo,[5,6,*] and Bong-Kiun Kaang[1,6,9,*]

[1]School of Biological Sciences, Seoul National University, 1 Gwanangno, Gwanak-gu, Seoul 08826, South Korea
[2]Max Planck Institute of Psychiatry, Department of Translational Research in Psychiatry, Kraepelinstr. 2, 80804 Munich, Germany
[3]Department of Dental Anesthesiology and Dental Research Institute, School of Dentistry, Seoul National University, Seoul 03080, South Korea
[4]Centre for Synaptic Plasticity, School of Physiology, Pharmacology & Neuroscience, University of Bristol, Bristol BS8 1TD, UK
[5]Department of Physiology, Faculty of Medicine, University of Toronto, 1 King's College Circle, Toronto, ON M5S 1A8, Canada
[6]Center for Neuron and Disease, Frontier Institutes of Science and Technology, Xi'an Jiaotong University, Xi'an 710049, China
[7]Lunenfeld-Tanenbaum Research Institute, Mount Sinai Hospital, Toronto, ON M5G 1X5, Canada
[8]These authors contributed equally
[9]Lead Contact
*Correspondence: g.collingridge@utoronto.ca (G.L.C.), min.zhuo@utoronto.ca (M.Z.), kaang@snu.ac.kr (B.-K.K.)
https://doi.org/10.1016/j.celrep.2017.12.059

SUMMARY

Peripheral nerve injury can induce pathological conditions that lead to persistent sensitized nociception. Although there is evidence that plastic changes in the cortex contribute to this process, the underlying molecular mechanisms are unclear. Here, we find that activation of the anterior cingulate cortex (ACC) induced by peripheral nerve injury increases the turnover of specific synaptic proteins in a persistent manner. We demonstrate that neural cell adhesion molecule 1 (NCAM1) is one of the molecules involved and show that it mediates spine reorganization and contributes to the behavioral sensitization. We show striking parallels in the underlying mechanism with the maintenance of NMDA-receptor- and protein-synthesis-dependent long-term potentiation (LTP) in the ACC. Our results, therefore, demonstrate a synaptic mechanism for cortical reorganization and suggest potential avenues for neuropathic pain treatment.

INTRODUCTION

Cortical neuronal circuits reorganize in response to external stimuli. Studies have demonstrated cortical rewiring in the adult brain induced by peripheral injury or sensory stimulation (Buonomano and Merzenich, 1998; Jain et al., 1998; Merzenich et al., 1984; Zhuo, 2008). Amputation induces cortical rewiring and synaptic plasticity (Kang et al., 2012; Kuner and Flor, 2016; Merzenich et al., 1984). In addition, sensory experiences and motor learning alter spine formation, elimination, and maturation in the visual, somatosensory, and motor cortices (Holtmaat et al., 2006; Majewska and Sur, 2003; Sarowar et al., 2016; Trachtenberg et al., 2002; Tropea et al., 2010; Xu et al., 2009; Yang et al., 2009; Yu et al., 2013; Yu and Zuo, 2011; Zuo et al., 2005). However, the molecular mechanisms involved in cortical synaptic reorganization following peripheral nerve injury are unclear.

Synaptic activity regulates protein synthesis and degradation, which contributes to cortical plasticity (Bingol et al., 2010; Jarome and Helmstetter, 2014; Rosenberg et al., 2014). Not only are ribosomes and proteasomes localized in dendrites and spines for local synthesis and degradation of synaptic proteins, but they also translocate to spines following synaptic activity (Bingol and Schuman, 2006; Bingol et al., 2010; Ostroff et al., 2002). For example, turnover of the scaffolding proteins, Shank and GKAP, increases following memory reactivation to induce memory retrieval and reconsolidation (Lee et al., 2008). Proteomics has identified synaptic proteins that increase or decrease after sensory deprivation, which suggests that the regulation of particular key proteins requires sensory experience (Butko et al., 2013).

Although synaptic activity can regulate synaptic protein turnover, it remains unclear whether this activity-induced turnover regulates cortical reorganization following a pathological condition and impacts synaptic structure, function, and behavior. Nerve injury, amputation, and inflammation, which all result in chronic pain, are known to induce plastic changes in the anterior cingulate cortex (ACC). In cortical areas, including the ACC, peripheral injuries cause long-term potentiation of synaptic responses, which is a cellular mechanism of chronic pain (Bliss et al., 2016; Chen et al., 2014; Descalzi et al., 2009; Kang et al., 2012; Li et al., 2010; Wei et al., 1999; Wei and Zhuo, 2001; Xu et al., 2008; Zhuo, 2008). Although there is evidence that translational regulation is important for nociception processing in peripheral neurons (Melemedjian et al., 2010; Moy et al.,

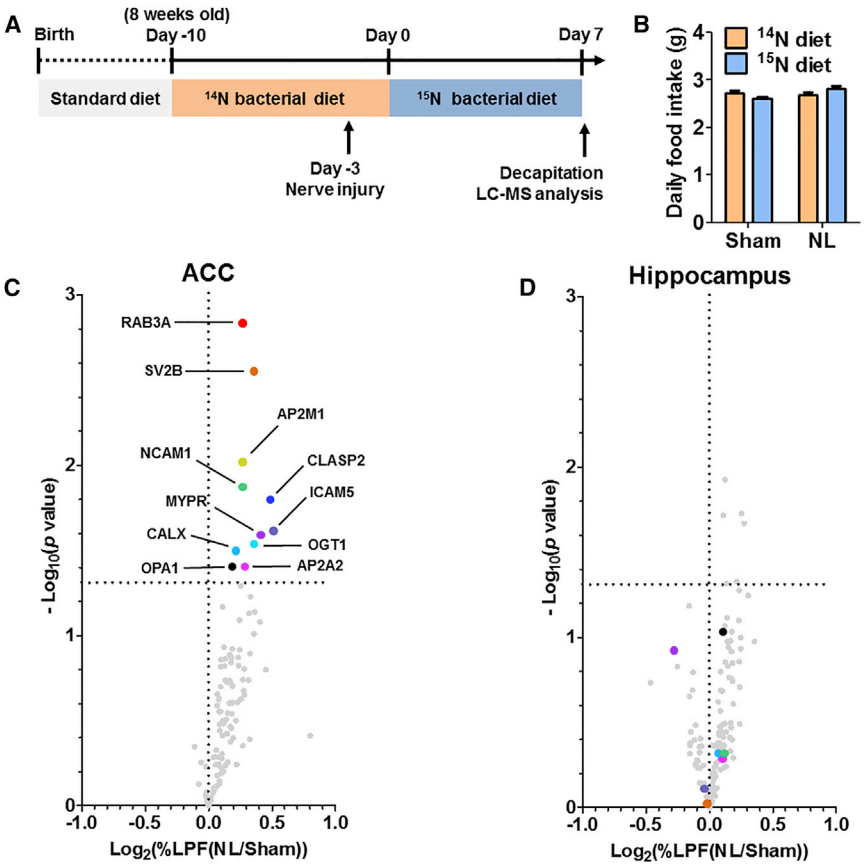

Figure 1. Peripheral Nerve Injury Enhances Turnover of Specific Proteins in the ACC

(A) Experimental scheme of LC-MS analysis using a ^{15}N diet. To adapt to the bacterial diet, mice were fed a ^{14}N bacterial diet for 1 week before nerve injury. Three days after surgery, the diet was switched with a ^{15}N bacterial diet. The ACC and hippocampus were dissected 1 week after ^{15}N diet consumption and used for LC-MS analysis.

(B) Mice did not show any preference between diets. Daily food consumption: n = 4 mice, two-way ANOVA followed by Bonferroni posttest; effect of diet, $F_{(1, 12)} = 0.02824$, $p > 0.05$; effect of surgery, $F_{(1, 12)} = 2.417$, $p > 0.05$; interaction, $F_{(1, 12)} = 4.238$, $p > 0.05$. Data are represented as mean ± SEM. NL, nerve ligation.

(C and D) Volcano plot of fold change of percent labeled peptide fraction (LPF) for each protein in the ACC (C) and hippocampus (D). Proteins with $-\log_{10}$ (p value) > 1.301 were considered significant (n = 3 or 4 mice, unpaired t test). AP2A2, AP-2 complex subunit alpha-2; AP2M1, AP-2 complex subunit mu; CALX; calnexin; CLASP2, CLIP-associating protein 2; ICAM5, intercellular adhesion molecule 5; MYPR, myelin proteolipid protein; NCAM1, neural cell adhesion molecule 1; OGT1, UDP-N-acetylglucosamine-peptide N-acetylglucosaminyltransferase, 110-kDa subunit; OPA1, dynamin-like 120-kDa protein, mitochondrial; RAB3A, Ras-related protein Rab-3A; SV2B, synaptic vesicle glycoprotein 2B.

See also Table S1.

2017), it is not known whether protein synthesis and/or degradation in higher centers is necessary for behavioral sensitization and cortical re-wiring. Here, we show that, following peripheral nerve injury, protein turnover in the ACC increases in a persistent manner. We identify NCAM1 as one of the critical molecules involved and have found that the mechanism of central sensitization resembles that underlying NMDA-receptor-dependent long-term potentiation (LTP) in the ACC.

RESULTS

Peripheral Injury Induces Active Protein Turnover in the ACC

We examined the protein turnover rate in the ACC during peripheral nerve injury. We compared the portion of newly synthesized proteins to preexisting proteins using mass spectrometric analysis of the ACC protein extracts from mice given an ^{15}N diet. After this dietary consumption, crude synaptosomal P2 fractions from the ACC and hippocampus from mice with either nerve injury, induced by nerve ligation, or sham surgery were analyzed by liquid chromatography-mass spectrometry (LC-MS) (Figure 1A). The groups did not show any difference in daily food consumption (Figure 1B). Using proteomic profiling analysis, we detected labeled peptide fractions of 111 proteins and identified 11 synaptic proteins that showed enhanced turnover rates in the ACC following peripheral nerve injury (Figure 1C; Table S1). These same proteins were either not detected or unaltered in the hippocampus, a brain region unrelated to nociception processing (Figure 1D; Table S1).

Increased Protein Synthesis Supports Structural Changes Induced by Peripheral Injury

Since we found that peripheral nerve injury induces rapid turnover of specific synaptic proteins, we examined whether altered protein turnover in the ACC supports synaptic structural changes induced by peripheral nerve injury. We used fosGFP transgenic mice to specifically investigate the structural properties of spines of activated neurons, 4 days after peripheral nerve ligation, a time point within the range of the proteomic screening to investigate the structural outcome that may be related to the increased turnover (Barth et al., 2004; Li et al., 2010). In this transgenic mouse line, the promoter of activity-dependent gene *c-fos* drives the expression of the truncated c-Fos and GFP fusion protein (fosGFP). This allows the visualization of activated neurons. We first confirmed that peripheral nerve injury indeed activates neurons in the ACC, as shown by the increased number of endogenous c-Fos-positive cells compared to the sham group, and that the majority of the fosGFP-positive cells simultaneously express endogenous c-Fos (Figure S1). We microinjected either vehicle (artificial cerebrospinal fluid [aCSF]) or anisomycin (protein synthesis inhibitor) dissolved in aCSF into the ACC 2 hr before decapitation and prepared slices from

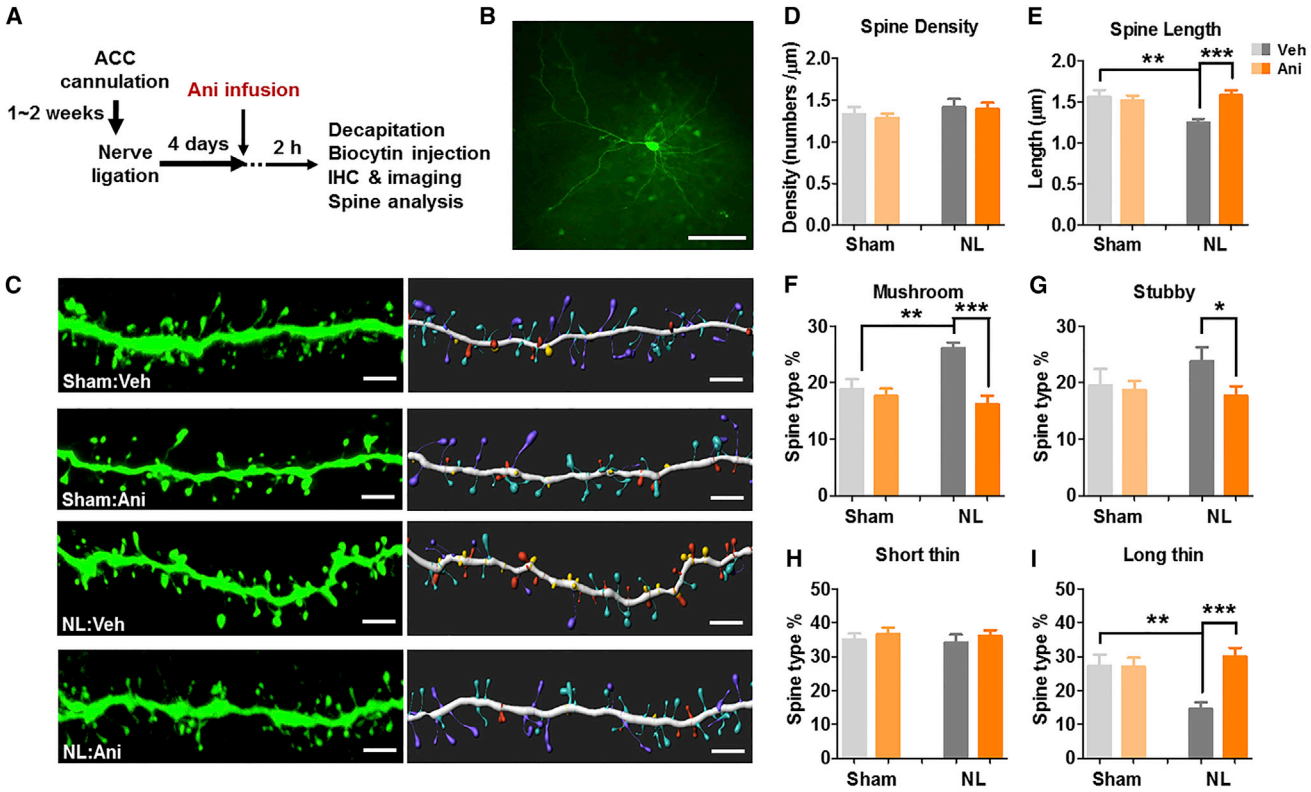

Figure 2. Nerve Injury Affects ACC Spine Morphology in a Protein-Synthesis-Dependent Manner

(A) Experimental scheme of spine analysis in the ACC after nerve injury. Four days after nerve ligation, Ani was microinjected into the ACC of fosGFP mice through an implanted cannula. Mice were decapitated 2 hr after Ani microinjection, and brain slices were prepared for biocytin injection. Biocytin-containing cells were immunostained to visualize and analyze spine morphology. IHC, immunohistochemistry.

(B) Sample biocytin-staining image at low magnification. Scale bar, 100 μm.

(C) Sample biocytin-staining images at high magnification. Left panels show raw fluorescence images. To clearly show spine types, raw images were reconstructed using the Imaris program (right panels). Yellow indicates stubby spine; red indicates mushroom spine; cyan indicates short thin spine; purple; indicates long thin spine. Scale bars, 3 μm.

(D–I) Total spine density, spine length, and percentage of spine types (Sham:Veh, n = 11 neurons; Sham:Ani, n = 17 neurons; NL:Veh, n = 13 neurons; and NL:Ani, n = 17 neurons; two-way ANOVA followed by Bonferroni posttest). NL, nerve ligation; Veh, vehicle (aCSF); Ani, anisomycin.

(D) Ani treatment and nerve injury did not alter total spine density: effect of drug, $F_{(1, 54)} = 0.1506$, $p > 0.05$; effect of surgery, $F_{(1, 54)} = 1.598$, $p > 0.05$; interaction, $F_{(1, 54)} = 0.01446$, $p > 0.05$.

(E) Nerve injury shortened average spine length. Ani treatment restored spine length after nerve injury: effect of drug, $F_{(1, 54)} = 5.090$, $p < 0.05$; effect of surgery, $F_{(1, 54)} = 3.789$, $p > 0.05$; interaction, $F_{(1, 54)} = 8.515$, $p < 0.01$; posttest, $^{**}p < 0.01$ and $^{***}p < 0.001$.

(F) The percentage of mushroom spines was enhanced by nerve injury and returned to basal levels after Ani treatment: effect of drug, $F_{(1, 54)} = 14.41$, $p < 0.001$; effect of surgery, $F_{(1, 54)} = 3.846$, $p > 0.05$; interaction, $F_{(1, 54)} = 8.737$, $p < 0.01$; posttest, $^{**}p < 0.01$ and $^{***}p < 0.001$.

(G) Ani reduced the percentage of stubby spines following nerve injury: effect of drug, $F_{(1, 54)} = 3.101$, $p > 0.05$; effect of surgery, $F_{(1, 54)} = 1.635$, $p > 0.05$; interaction, $F_{(1, 54)} = 2.912$, $^{*}p > 0.05$.

(H) The percentage of short thin spines was unaffected by nerve injury and Ani treatment: effect of drug, $F_{(1, 54)} = 0.8334$, $p > 0.05$; effect of surgery, $F_{(1, 54)} = 0.1152$, $p > 0.05$; interaction, $F_{(1, 54)} = 0.005465$, $p > 0.05$.

(I) The percentage of long thin spines was reduced by nerve injury and returned to basal levels after Ani treatment: effect of drug, $F_{(1, 54)} = 7.867$, $p < 0.01$; effect of surgery, $F_{(1, 54)} = 3.402$, $p > 0.05$; interaction, $F_{(1, 54)} = 8.575$, $p < 0.01$; posttest, $^{**}p < 0.01$ and $^{***}p < 0.001$).

Data are represented as mean ± SEM.

See also Figure S1.

sham or nerve ligation groups. FosGFP (+) neurons located in layer II/III in bilateral ACC were filled with biocytin. Then, we imaged secondary and tertiary labeled apical dendrites stained with biocytin and analyzed their neuronal spine properties (Figures 2A–2C). We found that nerve injury did not affect spine density, even after anisomycin injection into the ACC (Figure 2D). However, spine length decreased after nerve injury, and this effect was reversed by anisomycin (Figure 2E). We next classified spines into four types: stubby, mushroom, short thin, and long thin spines. The proportion of mushroom spines was significantly increased by peripheral nerve injury, an effect fully reversed by anisomycin (Figure 2F). Anisomycin also significantly reduced the proportion of stubby spines in those subjects that received nerve injury (Figure 2G). Although the proportion of short thin spines was unaltered (Figure 2H), the proportion of long thin spines decreased in an anisomycin-sensitive manner (Figure 2I).

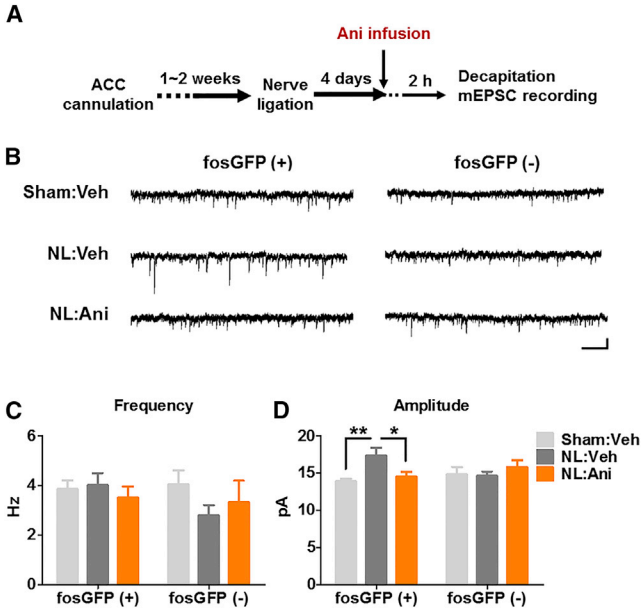

Figure 3. Nerve Injury Enhances Synaptic Transmission in a Protein-Synthesis-Dependent Manner in the ACC

(A) Experimental scheme of mEPSC recording in the ACC after nerve injury. Four days after nerve ligation, Ani was microinjected in the ACC of fosGFP mice through an implanted cannula. Mice were decapitated 2 hr after Ani microinjection, and brain slices were used for mEPSC recording.

(B) mEPSC recording sample traces. Scale bar represents 20 pA, 0.5 s.

(C and D) Frequency and amplitude of mEPSCs recorded from fosGFP (+) and fosGFP (−) neurons in fosGFP transgenic mice: Sham:Veh, n = 12 fosGFP (+) and 13 fosGFP (−) neurons from 8 mice; NL:Veh, n = 12 fosGFP (+) and 11 fosGFP (−) neurons from 7 mice; NL:Ani, n = 16 fosGFP (+) and 11 fosGFP (−) neurons from 7 mice. NL, nerve ligation; Veh, vehicle (aCSF); Ani, anisomycin.

(C) Frequency shows no significant difference among groups. Two-way ANOVA: effect of drug/surgery, $F_{(2, 67)} = 0.7030$, $p > 0.05$; effect of fosGFP expression, $F_{(1, 67)} = 0.8552$, $p > 0.05$; interaction, $F_{(2, 67)} = 0.9552$, $p > 0.05$.

(D) Peripheral nerve injury significantly increased mEPSC amplitude in fosGFP (+) neurons that was reversed by Ani treatment. There were no significant differences between groups in fosGFP (−) neurons. Two-way ANOVA followed by Bonferroni posttest: effect of drug/surgery, $F_{(2, 67)} = 2.120$, $p > 0.05$; effect of fosGFP expression, $F_{(1, 67)} = 0.04929$, $p > 0.05$; interaction, $F_{(2, 67)} = 3.798$, $p < 0.05$; posttest, $^{*}p < 0.05$ and $^{**}p < 0.01$.

Data are represented as mean ± SEM.

See also Figure S2.

Anisomycin had no significant effect in any of the sham groups. These results demonstrate that peripheral nerve injury alters spine morphology in the ACC in a manner that would be expected to strengthen neuronal activity. Surprisingly, this effect requires ongoing protein synthesis in order to maintain the altered morphological changes.

Increased Protein Synthesis Strengthens Synaptic Transmission Induced by Peripheral Injury

We have previously demonstrated that peripheral nerve injury enhances glutamatergic synaptic transmission in the ACC, specifically in stimulus-activated neurons (Li et al., 2010). If peripheral-injury-induced enhancement of synaptic transmission is mediated by protein turnover, then the inhibition of protein synthesis should decrease this enhanced responsivity in the ACC. To test this, we used fosGFP transgenic mice to examine synaptic properties (mEPSC [miniature excitatory postsynaptic current] frequency and amplitude) in neurons specifically affected by peripheral nerve injury (Figure 3A). We found that mEPSC amplitude, but not mEPSC frequency, increased 4 days after nerve ligation and that this effect was fully reversed by anisomycin treatment in the ACC (Figures 3B–3D). These effects were specific for fosGFP (+) neurons, since mEPSC frequency and amplitude were not significantly altered by nerve ligation and were not affected by anisomycin treatment in fosGFP (−) neurons. Furthermore, anisomycin had no effect on basal synaptic transmission (Figure S2). Taken together, these results demonstrate that peripheral nerve injury induces the persistent ongoing protein synthesis that is necessary for the enhanced synaptic strength.

LTP in the ACC Triggers Rapid Protein Turnover

Peripheral nerve injury induces an LTP-like state in the ACC (Bliss et al., 2016), which might be responsible for the increases in protein synthesis in this brain region. We stimulated layer V neurons in ACC slices using a theta burst stimulation (TBS) composed of three spaced bursts (inter-burst intervals of 10 min) (Figures 4A and 4B), which induced a persistent input-specific LTP that lasted unabatedly for at least 4 hr. A second TBS, delivered 140 min after the first ($+2^{nd}$ TBS), induced no additional LTP (Figures 4C and S3A), indicating that the initial 3xTBS (three episodes of TBS) had led to saturation of LTP. In the presence of anisomycin (25 μM), the second 3xTBS resulted in a decrease in responses toward basal levels (Figures 4D, 4E, and S3B). This is consistent with previous work in other brain region (Fonseca et al., 2006) that has shown that an LTP induction stimulus reactivates protein synthesis and that this is required to sustain the potentiation.

We reasoned that an activity-dependent increase in protein synthesis might be preceded by an activity-dependent increase in protein degradation to generate a labile state. To test this idea, we used a proteasome inhibitor, lactacystin (Lact, 10 nM), and found that this completely prevented the effects of anisomycin ("$+2^{nd}$ 3xTBS w/ anisomycin [Ani] + Lact" in Figures 4D, 4E, and S3B). These data indicate that repetitive synaptic activity induces a state in which LTP becomes vulnerable to protein synthesis inhibition (Okubo-Suzuki et al., 2016). The following results were also presented in a spatial manner, representing the percentage of certain channels of the MED64 electrodes showing activation (blue) or LTP (red) (Figures S3C–S3E). The spatial distribution of the activated channels was similar in all groups, but LTP showing channels in $+2^{nd}$ 3xTBS with the Ani group showed less potentiation compared to the other two groups (Figure S3D). This implies a lower percentage of the channel to show LTP. These results support the idea that increased protein turnover in the ACC in nerve-injured mice develops as a result of increased synaptic drive.

To establish the threshold of this effect, we applied weaker TBS protocols that were insufficient to induce LTP (1xTBS − 2^{nd} TBS and 0.6xTBS − 2^{nd} TBS in Figures 4A, 4C, and S3A). Compared to the standard TBS protocol of 3 episodes (each of 25 stimuli; 3xTBS) we delivered a single episode (of 25 stimuli; 1xTBS) and a partial episode (of 15 stimuli; 0.6xTBS). When these were given alone (at the second TBS time point), they did not affect the

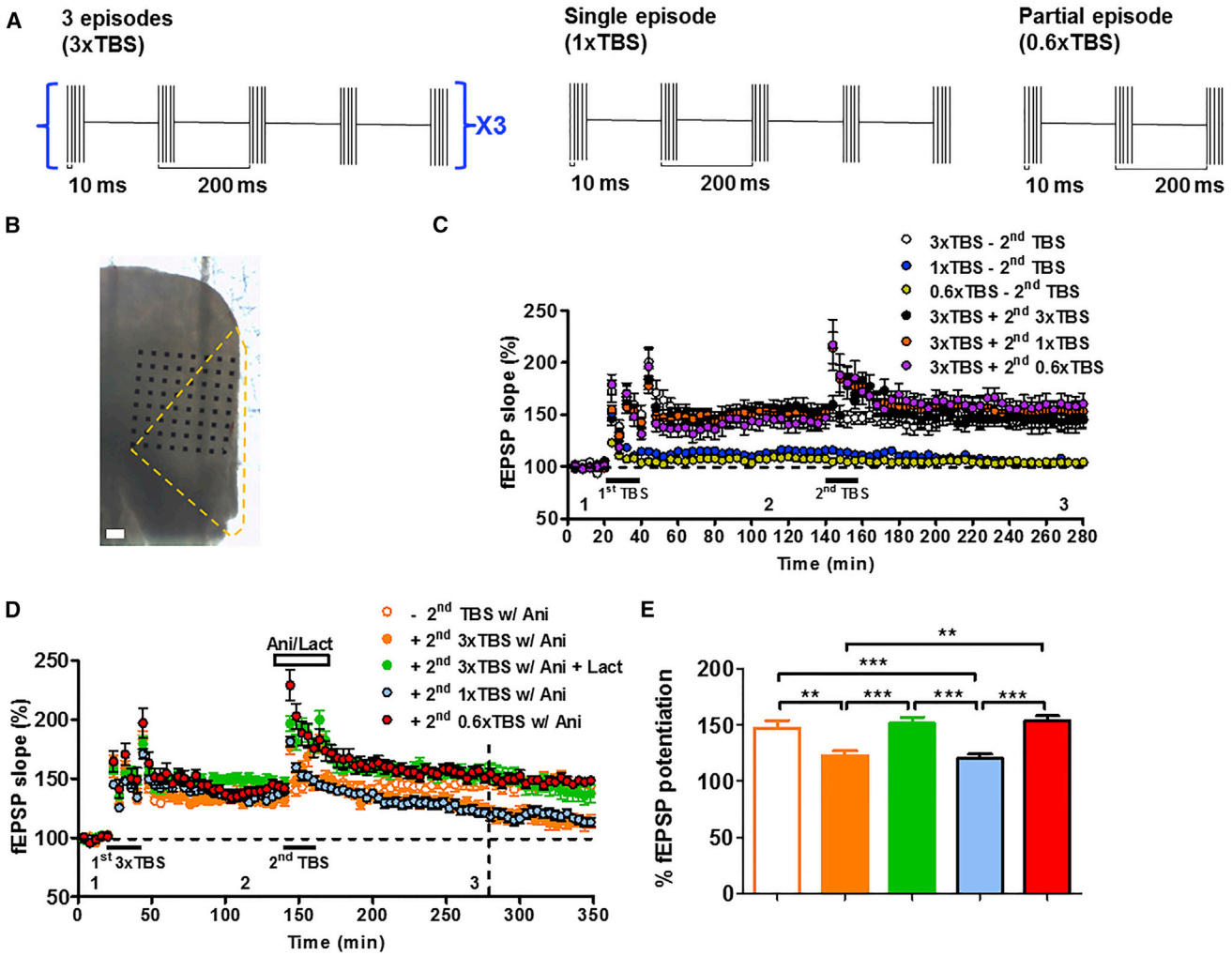

Figure 4. Reactivation of Protein Turnover by Spaced Theta-Burst Stimulation

(A) Stimulation protocols. Single episode comprised a burst of 5 shocks at 100 Hz delivered 5 times with an inter-burst interval of 200 ms. Three episodes were delivered with an inter-episode interval of 10 min.

(B) Sample image of ACC placement during MED64 recording. Scale bar, 200 μm.

(C) TBS comprising three bursts with an inter-burst interval of 10 min (3xTBS) induced LTP, while the weak TBSs (1xTBS and 0.6xTBS) failed to induce LTP. When these protocols were repeated 2 hr after the first 3xTBS, they did not induce additional LTP or disrupt the existing LTP (3xTBS − 2^{nd} TBS: n = 17 channels per 6 mice; 1xTBS − 2^{nd} TBS: n = 30 channels per 5 mice; 0.6xTBS − 2^{nd} TBS: n = 32 channels per 5 mice; 3xTBS + 2^{nd} 3xTBS: n = 30 channels per 6 mice; 3xTBS + 2^{nd} 1xTBS: n = 14 channels per 3 mice; 3xTBS + 2^{nd} 0.6xTBS: n = 14 channels per 3 mice).

(D) LTP was induced by 3xTBS. Bath application of Ani (25 μM) during the second 3xTBS reduced the potentiation level in LTP (+2^{nd} 3xTBS w/ Ani). In addition, weak stimulus (+2^{nd} 1xTBS w/ Ani) was enough to reduce the potentiation level of LTP when protein synthesis was blocked by Ani. However, there was a threshold of neural activity for maintaining active protein turnover. A stimulus weaker than 1xTBS (+2^{nd} 0.6xTBS w/ Ani) failed to disrupt LTP when Ani was applied: −2^{nd} TBS w/ Ani, n = 53 channels per 12 mice (0–280 min), and n = 18 channels per 12 mice (280–350 min); +2^{nd} 3xTBS w/ Ani, n = 46 channels per 12 mice (0–280 min), and n = 25 channels per 12 mice (280–350 min); +2^{nd} 3xTBS w/ Ani + Lact, n = 67 channels per 11 mice (0–280 min), and n = 47 channels per 11 mice (280–350 min); +2^{nd} 1xTBS w/ Ani, n = 102 channels per 11 mice (0–280 min), and n = 91 channels per 11 mice (280–350 min); +2^{nd} 0.6xTBS w/ Ani, n = 29 channels per 5 mice (0–280 min), and n = 20 channels per 5 mice (280–350 min). Ani, anisomycin; Lact, lactacystin.

(E) The percentage of fEPSP in (D) during the last 10 min of recording. The potentiation level differences were statistically significant: −2^{nd} TBS w/ Ani, 147.3 ± 6.737%; +2^{nd} 3xTBS w/ Ani, 122.9 ± 4.034%; +2^{nd} 3xTBS w/ Ani + Lact, 151.5 ± 5.372%; +2^{nd} 1xTBS w/ Ani, 120.3 ± 3.669%; +2^{nd} 0.6xTBS w/ Ani, 153.9 ± 4.318%; $p < 0.001$, one-way ANOVA followed by Newman-Keuls multiple comparison post hoc test. **$p < 0.01$; ***$p < 0.001$.

fEPSP, field excitatory postsynaptic potential. Data are represented as mean ± SEM. See also Figure S3.

maintenance of the LTP (3xTBS + 2^{nd} 1xTBS and 3xTBS + 2^{nd} 0.6x TBS in Figures 4A, 4C, and S3A). However, when they are applied in the presence of Ani, a single episode was able to decrease the response (+ 2^{nd} 1xTBS w/ Ani); in contrast, a partial episode was ineffective (+ 2^{nd} 0.6xTBS w/ Ani in Figures 4A, 4D, 4E, and S3B). These results imply that the threshold to induce the labile state in the ACC after peripheral nerve injury is lower than that required to induce LTP.

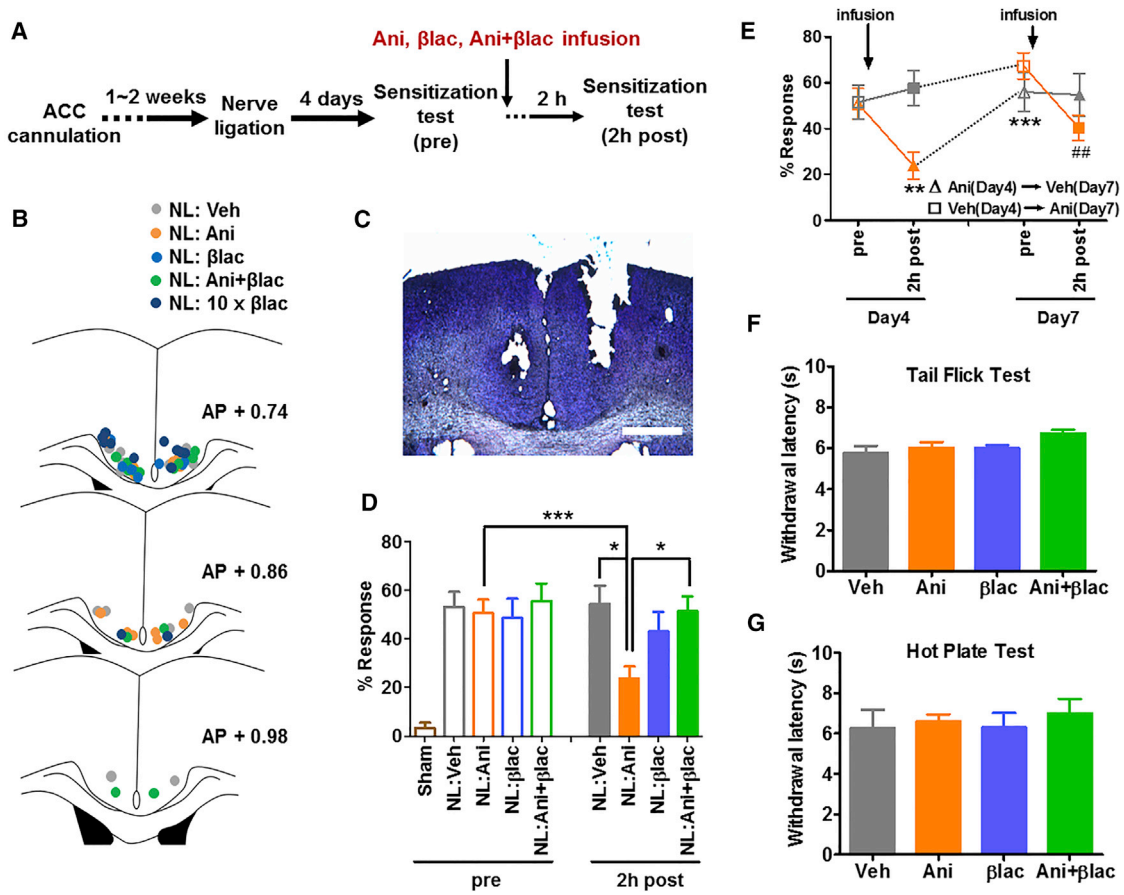

Figure 5. Maintenance of the Sensitized Response Requires Protein Turnover in the ACC

(A) Experimental scheme for testing the effects of Ani and/or β-lactone on the sensitized response to mechanical stimulation.

(B) Location of drug infusion sites in the ACC. NL, nerve ligation; Veh, vehicle (aCSF); Ani, anisomycin; βlac, β-lactone. AP, anterior posterior.

(C) Representative brain slice showing the microinjection site location. Scale bar, 50 μm.

(D) The mechanical sensitized response 2 hr after drug infusion (Ani, β-lactone, or Ani + β-lactone) into the ACC after nerve injury. Data were plotted as the percentage of sensitized responses in both hindpaws. n = 5–8 mice per group; NL group was analyzed using repeated-measures two-way ANOVA followed by Bonferroni posttest: effect of time, $F_{(1, 26)} = 15.10$, $p < 0.001$; effect of drug, $F_{(3, 26)} = 1.37$, $p > 0.05$; interaction, $F_{(3, 26)} = 6.99$, $p < 0.001$; posttest, *$p < 0.05$ and ***$p < 0.001$.

(E) The sensitized response was assessed before and after Ani or Veh infusion into the ACC on days 4 and 7. Mice with Ani injection on day 4 received Veh injection on day 7 and vice versa. The effect of Ani treatment assessed on day 4 had fully recovered by day 7. In contrast, Ani injection on day 7 was effective at inhibiting sensitization. n = 6 mice, repeated-measures one-way ANOVA followed by Tukey's posttest: Veh → Ani, $F_{(3, 15)} = 6.23$, $^{\#\#}p < 0.01$ (day 7 pre versus day 7 2 hr after injection [2h post]); Ani → Veh, $F_{(3, 15)} = 12.62$, **$p < 0.01$ (day 4 pre versus day 4 2h post) and ***$p < 0.001$ (day 4 2h post versus day 7 pre).

(F and G) Ani, β-lactone, or their co-administration into the ACC did not affect the withdrawal latency in the tail flick test (F) and hot plate test (G). n = 5–6 mice per group, one-way ANOVA; tail flick test, $F_{(3, 19)} = 2.74$, $p > 0.05$; hot plate test, $F_{(3, 19)} = 0.23$, $p > 0.05$.

Data are represented as mean ± SEM. See also Figure S4.

Sensitized Response Induced by Peripheral Injury Requires Active Protein Turnover in the ACC

Peripheral nerve injury can induce pathological conditions such as behavioral sensitization. We examined whether the active protein turnover in the ACC that we have identified underlies sensitized response following peripheral nerve injury. Mechanical sensitized responses were measured 4 days after nerve injury. Immediately after the first sensitization test ("pre" in Figures 5A and S4B), Ani or β-lactone (proteasome inhibitor) dissolved in aCSF was locally injected into the ACC, and sensitized responses were measured again 2 hr after drug infusion ("2h post" in Figures 5A and S4B). The microinjected sites are localized to the ventral part of ACC (Figures 5B and 5C). Nerve-injured mice displayed sensitized responses 4 days after peripheral nerve ligation. When the mice were tested before drug infusion, we detected no differences among groups; however, behavioral sensitization significantly decreased 2 hr after Ani injection into the ACC. Co-injection of β-lactone blocked this Ani effect (Figures 5D and S4E). Interestingly, β-lactone alone had no effect on sensitized response in nerve-injured mice, even when using high concentrations (Figures 5D and S4B). We found similar effects of Ani and β-lactone in a peripheral inflammation model using an injection of complete Freund's adjuvant (CFA) (Figures S4C and S4D).

In the peripheral nerve injury model, there is a persistent increase in neural activity within the ACC (Bliss et al., 2016). Therefore, we wondered whether the sensitized response would return after Ani diffuses away. To examine this possibility, we re-tested sensitized responses 3 days after the initial drug infusion (i.e., 7 days after nerve injury) (Figures 5E and S4F). On day 7, sensitized responses in Ani-injected mice had recovered to a level similar to that of the pretest level on day 4 (Ani → vehicle [Veh] group, orange filled triangle versus gray open triangle in Figure 5E). When Veh-injected mice on day 4 were injected with Ani in the ACC on day 7, they still showed reduced behavioral sensitization 2 hr after drug injection (Veh → Ani group, orange open square versus orange-filled square in Figures 5E and S4F). Ani injection itself did not have any effect on responses to acute noxious stimulus or on the basal mechanical threshold, suggesting that the effect of Ani is specific to chronic sensitized nociception rather that basal acute nociception (Figures 5F, 5G, and S4G). Taken together, these results show that active protein turnover in the ACC underlies a pathological sensitized state induced by peripheral nerve injury.

Peripheral Nerve Injury Enhances NCAM1 Turnover in the ACC

Among the 11 identified proteins that exhibited rapid turnover in the ACC after nerve injury, we further investigated the role of specific targets that have known roles in synaptic morphology: CLIP-associating protein 2 (CLASP2), intercellular adhesion molecule 5 (ICAM5), and neural cell adhesion molecule 1 (NCAM1) (Figure 1). NCAM1, in particular, contributes to neurite outgrowth, spine formation, and neuron-neuron interactions (Dallérac et al., 2013). In addition, the *Aplysia* cell adhesion molecule (apCAM), the *Aplysia* homolog of NCAM, is downregulated and restored by neural activity (Mayford et al., 1992). We tested whether these candidate proteins, indeed, show rapid turnover in the ACC during nerve injury. Since higher turnover rate accompanies both higher protein synthesis and degradation rates, we assumed that blocking protein synthesis should lead to greater reduction of the protein level due to the increased degradation rate (Figure 6A). We infused Ani into the ACC 4 days after nerve ligation. After an additional 2 hr, we assayed levels of these proteins in the ACC by western blot analysis. We found that peripheral nerve ligation significantly enhanced NCAM1 levels in the postsynaptic density (PSD) fraction and that Ani reversed this effect (Figure 6B). A second protein synthesis inhibitor, cycloheximide, had a similar effect (Figure S5A). In contrast, CLASP2 and ICAM5 did not show any significant changes when tested either 4 days (Figures S5B and S5E) or 7 days (Figures S5C, S5D, S5F, and S5G) after nerve injury and were unaffected by Ani.

The active turnover of NCAM1 seems to be a synapse-specific event, as we did not find any alterations in NCAM1 levels in the total ACC fraction (Figure 6C). Interestingly, the increase in its turnover is only seen during the initial stage of sensitization, because NCAM1 levels had returned to basal levels 7 days after nerve ligation (Figure 6D), and Ani treatment did not alter NCAM1 levels at this time point (Figure 6E). We further examined NCAM1 turnover by measuring its degradation. We found that ubiquitinated NCAM1 levels in the ACC increased 3 days, but not 7 days, after nerve ligation (Figure 6F), confirming the time-dependent increase in NCAM1 turnover. Moreover, NCAM1 level in the ACC of nerve-injured mice had returned to basal level after Ani infusion, and β-lactone counteracted the effect of protein synthesis inhibition, showing the parallel changes to behavioral sensitization (Figures 5D and S5H). Finally, NCAM1 expression was not altered in the PSD fraction of the hippocampus (Figure S6A). Collectively, these results demonstrate that NCAM1 is actively synthesized and degraded locally in ACC synapses during a critical time window after nerve injury.

In order to determine whether synaptic inputs from the peripheral nerve injury are required to maintain the increased turnover of NCAM1, we tested the effect of a local anesthetic, QX-314, on the area of injury (Lim et al., 2007; Wei and Zhuo, 2001). QX-314 injected into the injured hindlimb 30–60 min beforehand did not prevent the reduction in NCAM1 expression caused by Ani treatment (Figure S6B), indicating that inputs from the nerve injury are not required for the sensitivity to protein synthesis inhibition. In contrast, direct microinjection of either an AMPA receptor antagonist, NBQX; an NMDA receptor antagonist, AP5; or a CaMKII inhibitor, KN93, was able to completely prevent the susceptibility to Ani (Figure 6G). These results suggest that ongoing synaptic activity within the ACC is required to sustain the protein synthesis dependence of NCAM1. These results support the notion that the underlying mechanism is a form of NMDA-receptor-dependent LTP within the ACC.

Rapid Turnover of NCAM1 in the ACC Enables Synaptic Structural Reorganization and Behavioral Sensitization Induced by Peripheral Nerve Injury

We tested whether blockade of NCAM1 synthesis mediated the effects of Ani on spine reorganization and behavioral sensitization induced by peripheral nerve injury using NCAM1 knockdown with shNCAM1-expressing adeno-associated virus (AAV). We expressed short hairpin (sh)NCAM1 together with GFP in cultured neurons while transfecting a sparse population of neurons with myristoylated tdTomato to visualize spine structures. We found that the percentage of mushroom spines was decreased and that the percentage of short thin spines was increased, whereas the percentages of other spine types and the total spine density were not changed when the NCAM1 was knockdown in cultured neurons (Figures 7A–7D; Figure S7). These changes of morphological composition induced by NCAM1 knockdown are similar to those observed with protein synthesis inhibition using Ani.

In order to examine whether NCAM1 in the ACC participates in behavioral sensitization induced by peripheral nerve injury, we infused shNCAM1-expressing AAVs into the ACC. Four weeks after AAV infusion, we found that NCAM1 levels decreased approximately 50% (Figures 7E and 7F). The sensitized response was significantly attenuated in the shNCAM1 group, compared to the shLacZ control group 4 days after nerve ligation. Seven days after nerve ligation, a tendency for decreased sensitized response still persisted, although this was not significantly different. NCAM1 knockdown itself did not affect the basal mechanical threshold (day 0) (Figure 7G). In summary, these results show that NCAM1 turnover in the ACC contributes to behavioral sensitization and spine reorganization during a critical period after nerve injury.

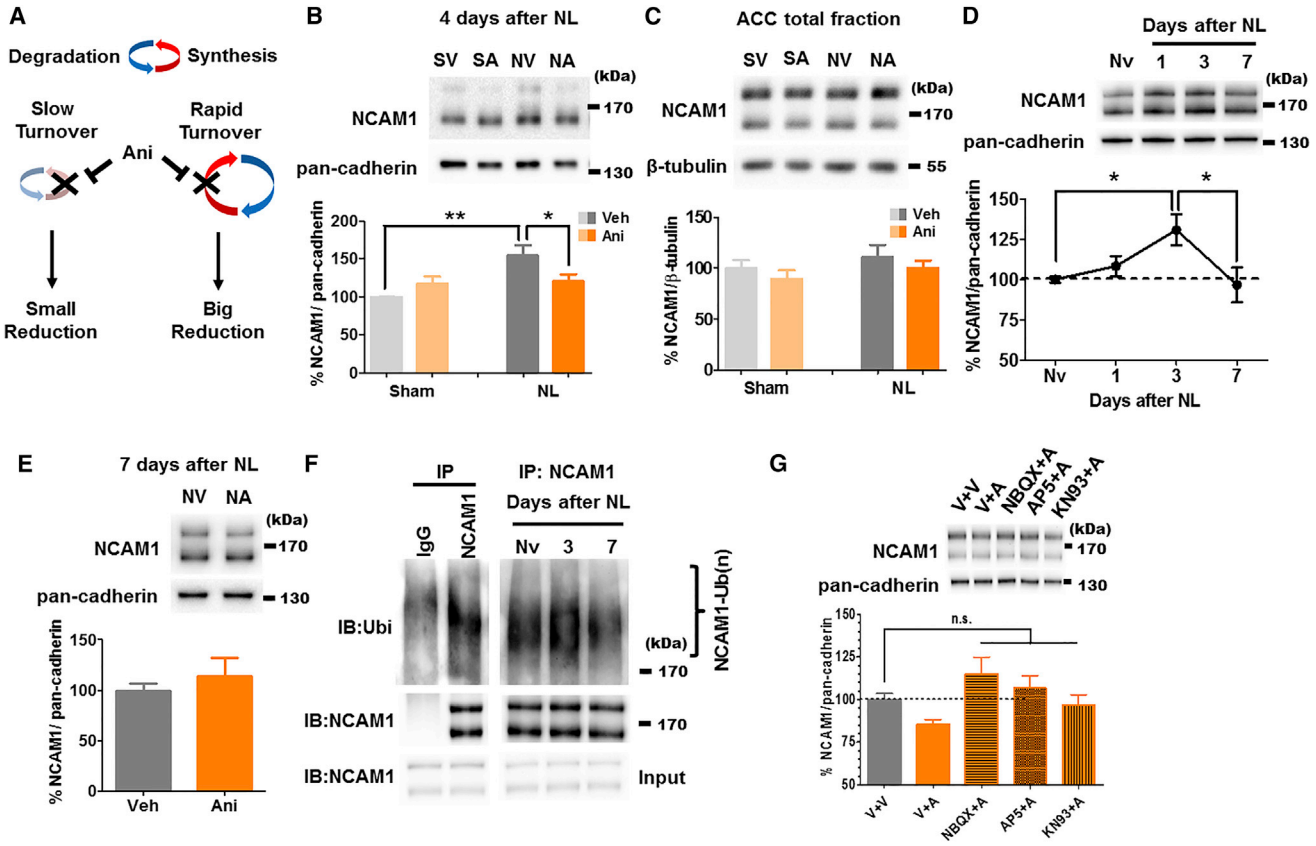

Figure 6. Peripheral Nerve Injury Enhances Protein Synthesis and Degradation of NCAM1 in the ACC

(A) A schematic view of protein turnover analysis using Ani.

(B) Peripheral nerve injury increased NCAM1 levels in the PSD from the ACC. Ani microinfusion into the ACC 4 days after nerve injury reduced NCAM1 levels only in the nerve injury group (n = 7 experimental trials; ACC slices from two mice were used for PSD fractionation; two-way ANOVA followed by Bonferroni posttest: effect of drug, $F_{(1, 24)} = 0.6902$, $p > 0.05$; effect of surgery, $F_{(1, 24)} = 8.745$, $p < 0.01$; interaction, $F_{(1, 24)} = 6.945$, $p < 0.05$; posttest, *$p < 0.05$ and **$p < 0.01$). NL, nerve ligation; SV, Sham+Veh; SA, Sham+Ani; NV, nerve injury+Veh; NA, nerve injury+Ani. aCSF was used for Veh.

(C) Ani treatment did not affect NCAM1 levels from the ACC total fraction in either sham or nerve injury groups (n = 7 mice per group; two-way ANOVA: effect of drug, $F_{(1, 24)} = 1.278$, $p > 0.05$; effect of surgery, $F_{(1, 24)} = 1.294$, $p > 0.05$; interaction, $F_{(1, 24)} = 0.001622$). SV, Sham+Veh; SA, Sham+Ani; NV, nerve injury+Veh, NA, nerve injury+Ani. aCSF was used for Veh.

(D) Time course of altered NCAM1 expression in the PSD of the ACC after nerve injury (n = 12 experimental trials; ACC slices from two mice were used for PSD fractionation; one-way ANOVA followed by Tukey's multiple comparison test: $F_{(3, 44)} = 3.759$, $p < 0.05$; posttest, *$p < 0.05$). NL, nerve ligation.

(E) Ani treatment did not reduce NCAM1 levels in the PSD of the ACC 7 days after nerve injury (n = 9 experimental trials; ACC slices from two mice were used for PSD fractionation; unpaired t test: $t_{(16)} < 1$, $p > 0.05$). NV, nerve injury+Veh; NA, nerve injury+Ani.

(F) The enhancement of ubiquitinated NCAM1 level 3 days after nerve injury. Experiments were replicated 3 times. IP, immunoprecipitation; Nv, naive.

(G) AMPA receptor, NMDA receptor, and CaMKII mediate active turnover of NCAM1 induced by the peripheral nerve injury. When AMPA receptor antagonist NBQX (6 μg/μL, 0.5 μL per side), NMDA receptor antagonist AP5 (0.4 μg/μL, 0.5 μL per side), or CaMKII inhibitor KN93 (10 μg/μL, 0.5 μL per side) was microinjected into the ACC 0–30 min before the Ani microinjection, the level of NCAM1 was not reduced by Ani (n = 13–17 experimental trials; ACC slices from two mice were used for PSD fractionation; $p < 0.05$, Kruskal-Wallis test followed by Dunn's multiple comparison test).

Data are represented as mean ± SEM. See also Figures S5 and S6.

DISCUSSION

We have found that peripheral nerve injury increases protein turnover of specific synaptic proteins in the ACC. This active protein turnover during nerve injury is required for the changes in spine morphology, increased synaptic strength, and behavioral sensitization. Through proteomic analysis, we identified 11 putative target proteins showing rapid turnover in the ACC after peripheral nerve injury. We revealed that active turnover of NCAM1, a protein that regulates synaptogenesis, neurite outgrowth, cell-cell interaction, and synaptic plasticity (Dallérac et al., 2013), in the ACC promotes structural and functional changes induced by nerve injury.

Memory formation involves experience-dependent structural and functional synaptic changes, which requires *de novo* protein synthesis during this process. However, after it is created, the memory becomes insensitive to protein synthesis inhibition (Carew and Sutton, 2001; Dudai, 2004). In contrast, in the peripheral nerve injury model, we demonstrated that active protein synthesis is continually required to maintain the structural and

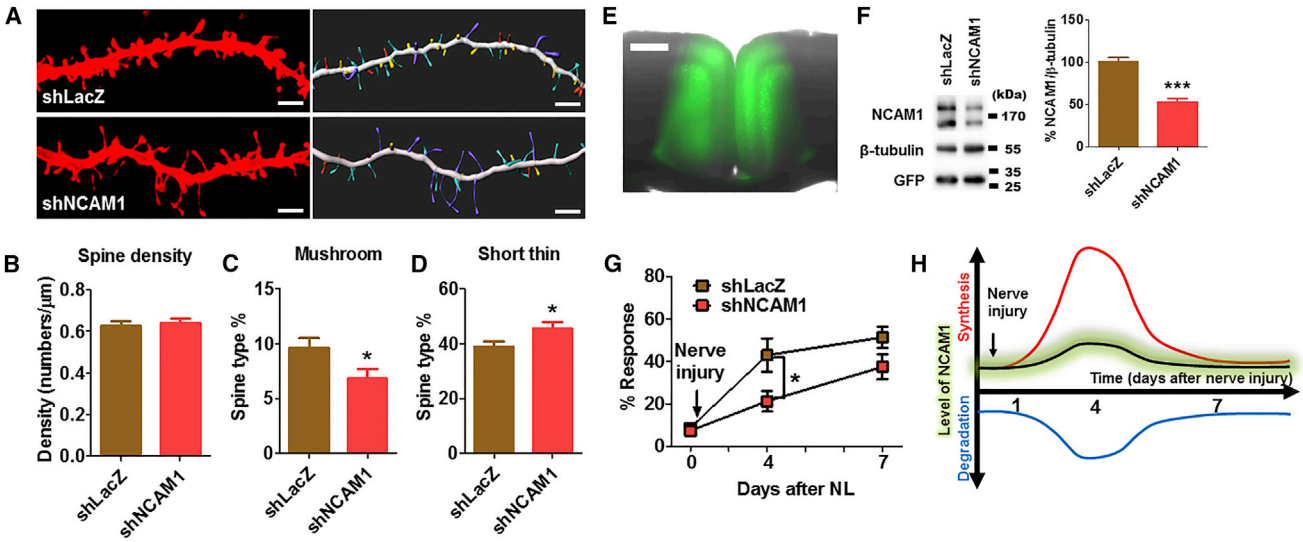

Figure 7. Rapid Turnover of NCAM1 in the ACC Contributes to Behavioral Sensitization to Peripheral Nerve Injury

(A) Representative spine image (left panels) of a cultured neuron transfected by shLacZ or shNCAM1 expressing AAV. To clearly show spine types, raw images were reconstructed by using the Imaris program (right panels). Yellow indicates stubby spine; red indicates mushroom spine; cyan indicates short thin spine; purple indicates long thin spine. Scale bars, 3 μm.

(B) NCAM1 knockdown did not affect total spine density (n = 47 neurons for shLacZ, and n = 44 neurons for shNCAM1); unpaired t test, $t_{(89)} < 1$, $p > 0.05$.

(C) NCAM1 knockdown reduced the percentage of mushroom spines, $t_{(89)} = 2.201$, $^{*}p < 0.05$.

(D) NCAM1 knockdown increased the percentage of short thin spines, $t_{(89)} = 2.179$, $^{*}p < 0.05$.

(E) Representative image of the ACC expressing shRNA (shLacZ or shNCAM1) and GFP. Scale bar, 50 μm.

(F) shNCAM1 expressing AAV efficiently reduced NCAM1 expression in the ACC. n = 12 mice for each group; unpaired t test, $t_{(22)} = 7.034$, $^{***}p < 0.001$.

(G) Knockdown of NCAM1 reduced behavioral sensitization induced by peripheral nerve injury (n = 12 mice for each group; repeated-measures two-way ANOVA followed by Bonferroni posttest: effect of time, $F_{(2, 44)} = 40.51$, $p < 0.001$; effect of shRNA, $F_{(1, 44)} = 5.211$, $p < 0.05$; interaction, $F_{(2, 44)} = 3.126$, $p > 0.05$; posttest, $^{*}p < 0.05$).

(H) Both protein synthesis (red line) and degradation (blue line) of NCAM1 are increased after nerve injury. The altered balance of synthesis and degradation leads to a net increase of NCAM1 level (black line), which returns to the basal level on day 7. Neuronal activity induces and maintains protein-synthesis- and degradation-dependent synaptic reorganization.

Data are represented as mean ± SEM. See also Figure S7.

functional synaptic changes to elicit the sensitized response. This sensitized response decreased following protein synthesis inhibition even a week after the surgery (Figure 5E). The reason for this striking difference between physiological memory formation and pathological behavioral sensitization is important to understand for therapeutic purposes. In this context, we have found that the upregulated protein turnover that is associated with sensitized nociception is accompanied by increased neuronal activity in the ACC (Figures 4 and S3). This important feature of peripheral nerve injury implies a continual retrieval and reconsolidation of nociceptive memories rather than a simple one-trial memory formation (Bliss et al., 2016). Reactivated memories undergo protein-degradation-dependent destabilization followed by a protein-synthesis-dependent restabilization process (Lee, 2008; Lee et al., 2008, 2012). Accordingly, we investigated the effects of β-lactone injection in conjunction with Ani and found that inhibition of protein degradation prevented the effects of protein synthesis inhibition. Therefore, the behavioral sensitization closely resembles memory reactivation studies, where β-lactone prevents the amnesic effect of Ani during reconsolidation, presumably by preventing the formation of the labile state.

Intriguingly, the structural and functional changes induced by nerve injury are maintained by an active increase in the synthesis and degradation of the same proteins. For NCAM1, the increased synthesis and degradation reaches a steady state where the overall NCAM1 level is slightly increased (Figures 6 and 7H). The rapid turnover of NCAM1, which is a critical protein that governs spine morphology (Figures 7A–7D), may lead to synaptic reorganization, which is manifest as a higher composition of mushroom spine and higher synaptic strength (Stewart et al., 2010). We assume that synthesis and degradation both occur in the same synapse in a relatively proportional level. It may be possible that specific spine type requires higher protein turnover rate than others for maintenance of its structure and function. In this model, protein synthesis inhibition will lead to the decrease of NCAM1 and, hence, a decrease in the proportion of mushroom spines (Figures 6 and 7). Proteasome inhibition can counteract the effect of protein synthesis inhibition on NCAM1 levels (Figure S5H).

We have found that behavioral sensitization is associated with increased synaptic activity in the ACC. This could be due to a constant afferent input driven by activity from the injured nerve or by an intrinsic change in higher structures. To test between the possibilities, we inhibited neural activity in the injured nerve using an established procedure (Lim et al., 2007; Wei and Zhuo, 2001) and found that this had no effect on the NCAM1

turnover. This implies that input from the periphery is not required for the persistent state. In contrast, we found that local injections of AMPA receptor, NMDA receptor, and CaMKII inhibitors directly into the ACC all inhibited the effect (Figure 6G). These findings clearly identify the ACC as a site of modification, though they do not exclude the involvement of other additional contributory circuits. Collectively, these findings suggest that there is altered synaptic activity in the ACC that, although initiated by the nerve-injury-induced neural activity, becomes self-sustaining even in the absence of continued sensory input. In terms of additional contributory factors, alterations in descending modulation after nerve injury may amplify sensory inputs from the periphery at the level of spinal cord, which can lead to altered inputs to the ACC neurons (Zhuo, 2016). In terms of the molecular mechanism that underlies the behavioral sensitization, the sensitivity to AMPAR, NMDAR and CaMKII inhibitors implicates an NMDAR-dependent LTP-like process. Consistent with this notion, we found that LTP in the ACC becomes sensitive to protein synthesis inhibition when reactivated by TBS and that this effect is counteracted by the inhibition of protein degradation.

Increased NCAM1 turnover contributes to behavioral sensitization during a critical time interval after peripheral nerve injury, while Ani was effective after this period (Figures 5E, 6, and 7E–7G). These data imply that different proteins may show increased turnover at later time points after peripheral nerve injury while NCAM1 is one of the critical target protein at an the earlier time point. The proteomic screening is a result of accumulated turnover for 7 days, including target proteins that show significant turnover change throughout the whole range or in a certain time point within this range. Among other target proteins, ICAM5 and CLASP2 (involved in stabilization of dynamic microtubule) could regulate spine architecture like NCAM1 (Matsuno et al., 2006; Schuyler and Pellman, 2001). We could not detect any significant decrease in the protein levels of ICAM5 and CLASP2 in western blot analysis after Ani treatment, which is possibly due to a compensation mechanism where protein synthesis inhibition has led to decreased protein degradation. Although we could not fully investigate other candidates due to lack of specific antibodies, our study clearly demonstrates that the proteomics allowed us to uncover a regulator of the sensitized state. Future studies will examine whether other proteins also show active turnover and specify how these proteins contribute to synaptic reorganization and behavioral sensitization induced by peripheral nerve injury in different time points.

In the present study, we found that elevated NCAM1 turnover supports structural and functional synaptic changes, which then induces a pathological state following nerve injury. In conclusion, our results provide pivotal insights into the mechanism of cortical synaptic reorganization induced by peripheral synaptic inputs. These findings indicate potential molecular targets for chronic pain.

EXPERIMENTAL PROCEDURES

Experimental Animals

Male wild-type C57BL/6NCrljBgi mice aged between 6 and 8 weeks were purchased from Charles River Laboratories or Orient Bio. FosGFP transgenic mice were purchased from Jackson Laboratory (stock #014135). Male mice aged over 8 weeks were used in all experiments. Animals were housed in standard laboratory cages on a 12-hr:12-hr light:dark cycle with access to food and water *ad libitum*. Mice were used for experiments 1–2 weeks after being housed in the laboratory cage. All the experiments were approved by the Institutional Animal Care and Use Committee of Seoul National University (SNU-150911-5-3, SNU-150413-1).

Behavioral Experiments

The mechanical sensitized response was measured 2 hr after drug infusion into ACC on day 4 or on days 4 and 7. Mice were acclimatized to an opaque round bucket (Figure S4A; diameter, 18 cm, height, 13 cm) around 1 hr prior to testing. Mechanical sensitized response was assessed based on the responsiveness of the hindpaw to the application of von Frey filaments (Stoelting, Wood Dale, IL, USA). The filament was applied over the dorsum of the foot while the animal was resting. In addition, the filament was approached carefully from the rear of mice to avoid false-positive responses. Based on previous experiments, we used a 1.65 filament to detect sensitized response (Vadakkan et al., 2005). Positive responses included licking, biting, and sudden withdrawal of the hindpaw. Nine trials were carried out every 5 min, and the results were expressed as a percentage of positive responses. For each time point, the percentage response frequency of hindpaw withdrawal was expressed as follows: (number of positive responses)/18 × 100 per hindpaw. After all experiments were finished, brains were used to check the location of the tip of the cannula (Figures 5B, 5C, and S4D). To measure response to an acute noxious stimulus, the latency of response to heating of the tail (tail-flick test) or to placement on a hot plate (55°C) was measured as described previously (Wu et al., 2005).

Spine Analysis in ACC Neurons

For biocytin labeling, slices were prepared similarly to those for mEPSC recording but with some modifications. The recording pipettes (3 to 5 MΩ) were filled with internal solution containing 145 K-gluconate, 5 mM NaCl, 0.2 mM EGTA, 10 mM HEPES, 2 mM MgATP, 0.1 mM Na_3GTP, 1 mM $MgCl_2$, 2 mg/mL biocytin ([pH 7.2] with KOH, 280 to 290 mOsm). The bath solution contained 124 mM NaCl, 2.5 mM KCl, 1 mM NaH_2PO_4, 25 mM $NaHCO_3$, 10 mM Glucose, 2 mM $CaCl_2$, 2 mM $MgSO_4$ saturated with 95% CO_2, 5% O_2. Coronal slices (300 μm) were prepared with the VT1000S microtome (Leica Microsystems). After incubation at room temperature (25°C to 26°C) for 1 hr, slices were transferred to a recording chamber (32°C to 34°C) perfused with oxygenated aCSF at a flow rate of 2 mL/min. GFP-positive pyramidal neurons in layer II/III were voltage clamped at −70 mV. After 15 min, the recording pipette was detached from the membrane, and the slice was fixed with 4% paraformaldehyde (PFA) overnight at 4°C. 1 to ~2 neurons per slice were labeled.

Fixed slices were washed three times with PBS shaking at 150 rpm and then were blocked and permeabilized with 5% goat serum, 0.2% Triton X-100 in PBS for 1 hr, at room temperature, while shaking at 80 rpm. Next, Streptavidin, Alexa Fluor 488 conjugate (Thermo Fisher Scientific) was diluted (1:2,000) in the same solution, and the slices were agitated overnight at 4°C. On the next day, slices were washed three times with PBS and mounted with VECTASHIELD Antifade Mounting Media (Vector Laboratories) on glass slides.

Labeled neurons were imaged by Zeiss LSM700 with a 100× oil immersion lens. Secondary/tertiary apical dendrites running horizontally to the coronal plane were imaged in z stack. Images were taken as stacks with 0.2-μm intervals. For each neuron, 100- to 300-μm segments of dendrites were imaged and analyzed, with several exceptional neurons with segments less than 100 μm analyzed due to the lack of clearly labeled, horizontal dendrites. The z stack images were reconstructed as 3D models and each parameter of the spines was measured using Imaris Filament Tracer (Bitplane). Spines were classified to four types: stubby, mushroom, long thin, or short thin. Stubby spines were defined as spines without a neck. Mushroom spines had a head width larger than 0.5 μm and a spine neck less than 0.5 μm. Spines that classified as neither stubby nor as mushroom spines were classified as long thin spines or short thin spines, with a cutoff of 2 μm in total spine length. Experimenters who injected biocytin and performed staining, imaging, and image analysis were all unaware of the nature of the experimental groups.

SUPPLEMENTAL INFORMATION

Supplemental Information includes Supplemental Experimental Procedures, seven figures, and one table and can be found with this article online at https://doi.org/10.1016/j.celrep.2017.12.059.

ACKNOWLEDGMENTS

This work was supported by two National Research Foundation (NRF) of Korea grants funded by the Korean government (MSIP) (NRF-2012R1A3A1050385 to B.-K.K. and 35B-2011-1-C00034 to H.-G.K.) and the Max Planck Society to C.W.T. J.-I.K., S.Y., and J.L. were supported by the BK21 Research Fellowship from the Ministry of Education, Science and Technology, Republic of Korea. M.Z. is supported by the Canadian Institute for Health Research (CIHR), Michael Smith Chair in Neurosciences and Mental Health, Canada Research Chair, a CIHR operating grant (MOP-124807) and a project grant (PJT-148648); the Azrieli Neurodevelopmental Research Program; and Brain Canada. G.L.C. is supported by the MRC (MR/K023098/1), Brain Canada, and the CIHR (154276).

AUTHOR CONTRIBUTIONS

H.-G.K. and J.-H.C. designed the studies, carried out the molecular and behavioral experiments, outlined the manuscript, and wrote the manuscript. D.I.P. performed quantitative protein turnover analysis. S.J.K., C.-S.L., S.-E.S., J.S., Siyong Kim, P.P., Somi Kim, and J.D. performed electrophysiological experiments. T.-H.C. analyzed spine change. J.-I.K. and S.Y. participated in western blot experiments. J.P. and J.L. participated in behavioral experiments. M.A.I. performed c-Fos immunohistochemistry. H.J.K., G.L.C., C.W.T., M.Z., and B.-K.K. supervised the experiments, participated in the interpretation of the data, and wrote the manuscript.

DECLARATION OF INTERESTS

The authors declare no competing interests.

Received: March 9, 2017
Revised: November 27, 2017
Accepted: December 17, 2017
Published: January 16, 2018

REFERENCES

Barth, A.L., Gerkin, R.C., and Dean, K.L. (2004). Alteration of neuronal firing properties after in vivo experience in a FosGFP transgenic mouse. J. Neurosci. *24*, 6466–6475.

Bingol, B., and Schuman, E.M. (2006). Activity-dependent dynamics and sequestration of proteasomes in dendritic spines. Nature *441*, 1144–1148.

Bingol, B., Wang, C.F., Arnott, D., Cheng, D., Peng, J., and Sheng, M. (2010). Autophosphorylated CaMKIIalpha acts as a scaffold to recruit proteasomes to dendritic spines. Cell *140*, 567–578.

Bliss, T.V., Collingridge, G.L., Kaang, B.K., and Zhuo, M. (2016). Synaptic plasticity in the anterior cingulate cortex in acute and chronic pain. Nat. Rev. Neurosci. *17*, 485–496.

Buonomano, D.V., and Merzenich, M.M. (1998). Cortical plasticity: from synapses to maps. Annu. Rev. Neurosci. *21*, 149–186.

Butko, M.T., Savas, J.N., Friedman, B., Delahunty, C., Ebner, F., Yates, J.R., 3rd, and Tsien, R.Y. (2013). In vivo quantitative proteomics of somatosensory cortical synapses shows which protein levels are modulated by sensory deprivation. Proc. Natl. Acad. Sci. USA *110*, E726–E735.

Carew, T.J., and Sutton, M.A. (2001). Molecular stepping stones in memory consolidation. Nat. Neurosci. *4*, 769–771.

Chen, T., Wang, W., Dong, Y.L., Zhang, M.M., Wang, J., Koga, K., Liao, Y.H., Li, J.L., Budisantoso, T., Shigemoto, R., et al. (2014). Postsynaptic insertion of AMPA receptor onto cortical pyramidal neurons in the anterior cingulate cortex after peripheral nerve injury. Mol. Brain *7*, 76.

Dallérac, G., Rampon, C., and Doyère, V. (2013). NCAM function in the adult brain: lessons from mimetic peptides and therapeutic potential. Neurochem. Res. *38*, 1163–1173.

Descalzi, G., Kim, S., and Zhuo, M. (2009). Presynaptic and postsynaptic cortical mechanisms of chronic pain. Mol. Neurobiol. *40*, 253–259.

Dudai, Y. (2004). The neurobiology of consolidations, or, how stable is the engram? Annu. Rev. Psychol. *55*, 51–86.

Fonseca, R., Nägerl, U.V., and Bonhoeffer, T. (2006). Neuronal activity determines the protein synthesis dependence of long-term potentiation. Nat. Neurosci. *9*, 478–480.

Holtmaat, A., Wilbrecht, L., Knott, G.W., Welker, E., and Svoboda, K. (2006). Experience-dependent and cell-type-specific spine growth in the neocortex. Nature *441*, 979–983.

Jain, N., Florence, S.L., and Kaas, J.H. (1998). Reorganization of somatosensory cortex after nerve and spinal cord injury. News Physiol. Sci. *13*, 143–149.

Jarome, T.J., and Helmstetter, F.J. (2014). Protein degradation and protein synthesis in long-term memory formation. Front. Mol. Neurosci. *7*, 61.

Kang, S.J., Liu, M.G., Chen, T., Ko, H.G., Baek, G.C., Lee, H.R., Lee, K., Collingridge, G.L., Kaang, B.K., and Zhuo, M. (2012). Plasticity of metabotropic glutamate receptor-dependent long-term depression in the anterior cingulate cortex after amputation. J. Neurosci. *32*, 11318–11329.

Kuner, R., and Flor, H. (2016). Structural plasticity and reorganisation in chronic pain. Nat. Rev. Neurosci. *18*, 20–30.

Lee, J.L. (2008). Memory reconsolidation mediates the strengthening of memories by additional learning. Nat. Neurosci. *11*, 1264–1266.

Lee, S.H., Choi, J.H., Lee, N., Lee, H.R., Kim, J.I., Yu, N.K., Choi, S.L., Lee, S.H., Kim, H., and Kaang, B.K. (2008). Synaptic protein degradation underlies destabilization of retrieved fear memory. Science *319*, 1253–1256.

Lee, S.H., Kwak, C., Shim, J., Kim, J.E., Choi, S.L., Kim, H.F., Jang, D.J., Lee, J.A., Lee, K., Lee, C.H., et al. (2012). A cellular model of memory reconsolidation involves reactivation-induced destabilization and restabilization at the sensorimotor synapse in Aplysia. Proc. Natl. Acad. Sci. USA *109*, 14200–14205.

Li, X.Y., Ko, H.G., Chen, T., Descalzi, G., Koga, K., Wang, H., Kim, S.S., Shang, Y., Kwak, C., Park, S.W., et al. (2010). Alleviating neuropathic pain hypersensitivity by inhibiting PKMzeta in the anterior cingulate cortex. Science *330*, 1400–1404.

Lim, T.K., Macleod, B.A., Ries, C.R., and Schwarz, S.K. (2007). The quaternary lidocaine derivative, QX-314, produces long-lasting local anesthesia in animal models in vivo. Anesthesiology *107*, 305–311.

Majewska, A., and Sur, M. (2003). Motility of dendritic spines in visual cortex in vivo: changes during the critical period and effects of visual deprivation. Proc. Natl. Acad. Sci. USA *100*, 16024–16029.

Matsuno, H., Okabe, S., Mishina, M., Yanagida, T., Mori, K., and Yoshihara, Y. (2006). Telencephalin slows spine maturation. J. Neurosci. *26*, 1776–1786.

Mayford, M., Barzilai, A., Keller, F., Schacher, S., and Kandel, E.R. (1992). Modulation of an NCAM-related adhesion molecule with long-term synaptic plasticity in Aplysia. Science *256*, 638–644.

Melemedjian, O.K., Asiedu, M.N., Tillu, D.V., Peebles, K.A., Yan, J., Ertz, N., Dussor, G.O., and Price, T.J. (2010). IL-6- and NGF-induced rapid control of protein synthesis and nociceptive plasticity via convergent signaling to the eIF4F complex. J. Neurosci. *30*, 15113–15123.

Merzenich, M.M., Nelson, R.J., Stryker, M.P., Cynader, M.S., Schoppmann, A., and Zook, J.M. (1984). Somatosensory cortical map changes following digit amputation in adult monkeys. J. Comp. Neurol. *224*, 591–605.

Moy, J.K., Khoutorsky, A., Asiedu, M.N., Black, B.J., Kuhn, J.L., Barragán-Iglesias, P., Megat, S., Burton, M.D., Burgos-Vega, C.C., Melemedjian, O.K., et al. (2017). The MNK-eIF4E signaling axis contributes to injury-induced nociceptive plasticity and the development of chronic pain. J. Neurosci. *37*, 7481–7499.

Okubo-Suzuki, R., Saitoh, Y., Shehata, M., Zhao, Q., Enomoto, H., and Inokuchi, K. (2016). Frequency-specific stimulations induce reconsolidation of long-term potentiation in freely moving rats. Mol. Brain *9*, 36.

Ostroff, L.E., Fiala, J.C., Allwardt, B., and Harris, K.M. (2002). Polyribosomes redistribute from dendritic shafts into spines with enlarged synapses during LTP in developing rat hippocampal slices. Neuron *35*, 535–545.

Rosenberg, T., Gal-Ben-Ari, S., Dieterich, D.C., Kreutz, M.R., Ziv, N.E., Gundelfinger, E.D., and Rosenblum, K. (2014). The roles of protein expression in synaptic plasticity and memory consolidation. Front. Mol. Neurosci. *7*, 86.

Sarowar, T., Grabrucker, S., Föhr, K., Mangus, K., Eckert, M., Bockmann, J., Boeckers, T.M., and Grabrucker, A.M. (2016). Enlarged dendritic spines and pronounced neophobia in mice lacking the PSD protein RICH2. Mol. Brain *9*, 28.

Schuyler, S.C., and Pellman, D. (2001). Microtubule "plus-end-tracking proteins": The end is just the beginning. Cell *105*, 421–424.

Stewart, M., Popov, V., Medvedev, N., Gabbott, P., Corbett, N., Kraev, I., and Davies, H. (2010). Dendritic spine and synapse morphological alterations induced by a neural cell adhesion molecule mimetic. Adv. Exp. Med. Biol. *663*, 373–383.

Trachtenberg, J.T., Chen, B.E., Knott, G.W., Feng, G., Sanes, J.R., Welker, E., and Svoboda, K. (2002). Long-term in vivo imaging of experience-dependent synaptic plasticity in adult cortex. Nature *420*, 788–794.

Tropea, D., Majewska, A.K., Garcia, R., and Sur, M. (2010). Structural dynamics of synapses in vivo correlate with functional changes during experience-dependent plasticity in visual cortex. J. Neurosci. *30*, 11086–11095.

Vadakkan, K.I., Jia, Y.H., and Zhuo, M. (2005). A behavioral model of neuropathic pain induced by ligation of the common peroneal nerve in mice. J. Pain *6*, 747–756.

Wei, F., and Zhuo, M. (2001). Potentiation of sensory responses in the anterior cingulate cortex following digit amputation in the anaesthetised rat. J. Physiol. *532*, 823–833.

Wei, F., Li, P., and Zhuo, M. (1999). Loss of synaptic depression in mammalian anterior cingulate cortex after amputation. J. Neurosci. *19*, 9346–9354.

Wu, L.J., Toyoda, H., Zhao, M.G., Lee, Y.S., Tang, J., Ko, S.W., Jia, Y.H., Shum, F.W., Zerbinatti, C.V., Bu, G., et al. (2005). Upregulation of forebrain NMDA NR2B receptors contributes to behavioral sensitization after inflammation. J. Neurosci. *25*, 11107–11116.

Xu, H., Wu, L.J., Wang, H., Zhang, X., Vadakkan, K.I., Kim, S.S., Steenland, H.W., and Zhuo, M. (2008). Presynaptic and postsynaptic amplifications of neuropathic pain in the anterior cingulate cortex. J. Neurosci. *28*, 7445–7453.

Xu, T., Yu, X., Perlik, A.J., Tobin, W.F., Zweig, J.A., Tennant, K., Jones, T., and Zuo, Y. (2009). Rapid formation and selective stabilization of synapses for enduring motor memories. Nature *462*, 915–919.

Yang, G., Pan, F., and Gan, W.B. (2009). Stably maintained dendritic spines are associated with lifelong memories. Nature *462*, 920–924.

Yu, X., and Zuo, Y. (2011). Spine plasticity in the motor cortex. Curr. Opin. Neurobiol. *21*, 169–174.

Yu, X., Wang, G., Gilmore, A., Yee, A.X., Li, X., Xu, T., Smith, S.J., Chen, L., and Zuo, Y. (2013). Accelerated experience-dependent pruning of cortical synapses in ephrin-A2 knockout mice. Neuron *80*, 64–71.

Zhuo, M. (2008). Cortical excitation and chronic pain. Trends Neurosci. *31*, 199–207.

Zhuo, M. (2016). Neural mechanisms underlying anxiety-chronic pain interactions. Trends Neurosci. *39*, 136–145.

Zuo, Y., Yang, G., Kwon, E., and Gan, W.B. (2005). Long-term sensory deprivation prevents dendritic spine loss in primary somatosensory cortex. Nature *436*, 261–265.